Journal of Nano- and Electronic Physics
Vol. **10** No 2, 02027(6pp) (2018)

Журнал нано- та електронної фізики
Том **10** № 2, 02027(6cc) (2018)

Comparative Study of Temperature Effect on Thin Film Solar Cells

Mahfoud Abderrezek[1,*], Mohamed Fathi[1,†], Farid Djahli[2,‡]

[1] *Unité de Développement des Equipements Solaires, UDES / Centre de Développement des Energies Renouvelables, CDER, 42415Tipaza, Algérie*
[2] *L.I.S Laboratory, Department of Electronics, Faculty of Technology, University of Setif 1, 19000, Setif, Algeria*

(Received 07 December 2017; published online 29 April 2018)

The quaternary compound Cu_2ZnSnS_4 (CZTS) is considered as an alternative material to replace CIGS material in future manufacturing of thin film solar cells. In this paper, a comparative study of temperature effect on thin film CZTS (Cu_2ZnSnS_4) and CIGS ($Cu(In, Ga)Se_2$) solar cells was leaded. For this purpose we used the one dimensional simulation program tool SCAPS-1D (Solar Cell Capacitance Simulator in one Dimension. The dependence of the CZTS and CIGS solar cells characteristics with temperature was investigated from 300°K to 360°K. The comparative results showed that the cell with CZTS had an improved behavior at high operation temperatures. The maximum power coefficients, depending on temperature variations, were respectively – 1.8 mW/cm² °K and – 7.84 mW/cm² °K.

Keywords: Thin film, Solar cells, Temperature, CZTS, CIGS, SCAPS-1D.

DOI: 10.21272/jnep.10(2).02027 PACS numbers: 68.60.Bs, 78.66.Bz

1. INTRODUCTION

Solar energy is the most promising and powerful energy source among renewable energies. It provides an alternative solution to conventional energies. It is a low cost, clean and environmentally friendly energy [1].

In recent years, thin-film solar cells have drawn great attention due to their promising performances. Also, they play a significant role in reducing the cost of manufacturing photovoltaic modules. Potential candidate for thin film solar cells materials are: CdTe, Cu (In, Ga) Se_2 (CIGS) and Si amorphous. For reasons of stability, respect for the environment and the displayed yields, the CIGS compounds are the most emerging and the most promising [2].

The CIGS solar cell has a high absorption coefficient ($\alpha > 10^5\,cm^{-1}$); its conversion efficiency reached 21 % in 2016 [3]. Also, it is considered as a semiconductor of future which will allow enhancing the conversion efficiency of III-V tandem solar cells, due to its band gap which can achieve 1eV. This value of band gap permits to this compound to play the role of a third junction in III-V tandem solar cells [4].

However, the use of relatively expensive and rare elements such as indium (In) and gallium (Ga), in the production of CIGS solar cells, limits the production of PV CIGS modules on a large scale [5].

On another hand, the quaternary compound Cu_2ZnSnS_4 (CZTS) has been intensively examined as an alternative solar cells material due to its similarity in material properties with CIGS and the relative abundance of raw materials [2, 6, 7]. The obtained results of Wadia et al. 2009 [8] indicate that the cost of raw material for a CZTS PV technology is much lower than that of the three existing thin film PV technologies (CIGS, CdTe, and thin film Si). Thin film CZTS is also nontoxic and is prepared on a low-cost substrate such as a glass plate, a metal sheet, or a plastic sheet [6]. Furthermore, due to the high absorption coefficient of the CZTS absorber ($\alpha > 10^4\,cm^{-1}$), its direct band gap of 1.5 eV [9] and the good adaptation between the maximum quantum efficiency of the materials and the maximum power of the terrestrial solar spectrum (AM1.5G) [10], this absorber is ranked among the best semiconductors used in the field of photovoltaic terrestrial, for power generation. Laboratory tests allowed obtaining average conversion efficiency of about 12.6 % [11].

In order to lead comparative tests between the performances of the new CZTS cell and those of the CIGS, the outdoor installation of the PV modules, in different locations, necessities to study their behavior with respect to temperature which can reach 63 °C in desert, during summer period [12]. The study of temperature effect on solar cells allows us to quantify thermal losses in the solar cell. This helps a choosing of the most suitable material in the manufacturing of the solar cell that ensures optimal operation under climatic conditions of the chosen site.

This work focuses on the simulation of CIGS and CZTS solar cells. The numerical solutions obtained by using solar cell capacitance simulator in one dimension (SCAPS-1D) will be used to improve solar cells performances [13].

The main objective of this research is also to study the behavior of CZTS and CIGS solar cells in high temperature condition and to select the best one (i.e. the one having less thermal losses).

2. MOTIVATION TEMPERATURE EFFECT ON SOLAR CELL ELECTRICAL PARAMETERS

The numerical calculations were performed by the SCAPS-1D V.2.9 simulator, developed with Lab Windows/CVI of National Instruments at University of

* mahfoud_cbi@yahoo.fr
† dr_fathimohamed@yahoo.fr
‡ fdjahli@yahoo.fr

Gent. It has a user-friendly program interface and includes in his data output the five main parameters essential to examine the behavior of solar cell. These parameters are: short circuit current density (JSC), open circuit voltage (VOC), fill factor (FF), conversion efficiency (η) and quantum efficiency (QE) [2].

The analysis of the semiconductors is based, essentially on the Poisson equation, conditions to the limits and electron- and hole-continuity equations. These are the basic equations who describe the different phenomena involved in most photovoltaic structures.

The Poisson equation links the variations of the electrostatic potential (electric field) to the local densities of load. It is expressed by [14]:

$$\frac{-\mathrm{d}^2\varphi}{dx^2} = \frac{dE}{dx} = \frac{\rho}{\varepsilon_r \varepsilon_0} \tag{1}$$

where ρ is the total electric load in the semiconductor, ε_0 and ε_r are respectively the permittivity under vacuum and the relative dielectric permittivity of materiel, φ is the electrostatic potential and n and p are the concentrations of the free carriers. The total electric load (ρ) is determined by the following equation:

$$\rho = q(p - n + N_D^+ - N_A^-) \tag{2}$$

Where N_D^+ and N_A^- are the densities of the ionized donors and acceptors.

The continuity equations permit to determine, in all point and in every instant, the concentration of the carriers in a semiconductor. They are expressed as follows:

$$\frac{\partial n}{\partial t} = \frac{1}{q} div\overrightarrow{J_n} + G_n - R_n \tag{3}$$

$$\frac{\partial p}{\partial t} = -\frac{1}{q} div\overrightarrow{J_p} + G_p - R_p \tag{4}$$

Where G_n and G_p are the optical generation rates of the electrons-holes pairs, R_n and R_p are respectively the rates of recombination for the electrons and the holes, $\overrightarrow{J_n}$ and $\overrightarrow{J_p}$ are the densities of the currents of the electrons and holes.

A solar cell, under real operating conditions, can be assimilated to a current generator in which the direct polarization or darkness current Jobs (reverse saturation current density) of the junction must be driven.

A solar cell circuit is composed of a current generator with two diodes representing the behavior of the cell at darkness junction PN (Fig. 1).

A mathematical model of the equivalent circuit of Fig. 1, is given by the following equations [6]:

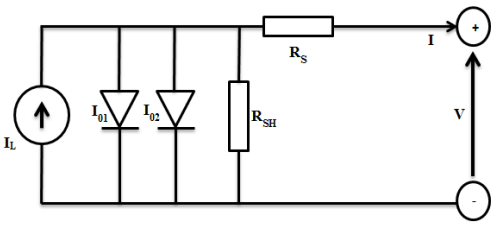

Fig. 1 – Equivalent circuit model for a real solar cell

$$J = J_L - J_{01}\left[\exp\left(\frac{q(V + JR_S)}{AK_BT}\right) - 1\right] - J_{02}\left[\exp\left(\frac{q(V + JR_S)}{A'K_BT}\right) - 1\right] - \left(\frac{(V + JR_S)}{R_{Sh}}\right), \tag{5}$$

where T is the absolute temperature in Kelvin, J_L is the photocurrent, J_{01} and J_{02} are the two saturation current densities, A and A' are the ideality factors of these diodes, R_s and R_{sh} are respectively the series and shunt resistances.

The open circuit voltage is given by:

$$V_{OC} = \frac{AK_BT}{q} ln\left[1 + {}^{J_L}\!/_{J_0}\right] \tag{6}$$

$J_0 = J_{01} + J_{02}$, is given as a function of temperature dependence:

$$Jo = BT^{3/n} exp({}^{-Eg}\!/_{mkT}) \tag{7}$$

Where B is an empirical parameter, k is Boltzmann's constant, m and n are empirical parameters depending on a dominating recombination mechanism in a solar cell.

A variation of the semiconductor band gap with a temperature is described by Varshni model [2]:

$$E_G\ (eV) = E_{g0} - {}^{\alpha T^2}\!/_{(T+\beta)} \tag{8}$$

Where α and β are the coefficients of band gap temperature dependence for the considered material and E_{g0} is the band gap energy at $T = 0$°K.

The fill factor FF_0 depends only on the quantity $v_{OC} = V_{OC}/KT$ as shown in equation (9):

$$FF_0 = {}^{(v_{CO} - \ln(v_{CO} + 0.72))}\!/_{(v_{CO} + 1)} \tag{9}$$

v_{CO} is the normalized open-circuit voltage defined as follows:

$$v_{CO} = \frac{nkT}{q} Voc \tag{10}$$

Where n is the diode ideality factor.

In real situations, the FF is very sensitive to parasitic resistances R_s and R_{sh} of a solar cell [2]:

$$FF = FF_0(1 - r_s) \tag{11}$$

$$r_s = R_S I_{CC} / V_{CO} \tag{12}$$

Finally, the conversion efficiency of the solar cell is given by:

$$\eta = {}^{Pout}\!/_{Pin} = {}^{V_{oc} \times J_{sc} \times FF}\!/_{Pin} \tag{13}$$

3. THE STUDIED STRUCTURE

The CZTS/CdS/ZnO and CIGS/CdS/ZnO structures have been considered for a comparative study of based

thin film photovoltaic devices. The two solar cells are formed by a similar Transparent Conductive Oxide (ZnO) and a same Buffer (CdS) materials but with different absorber materials (CZTS, CIGS). The window layer must be both conductive and transparent, so as to collect the electrons while letting the light pass. This layer consists of a conductive transparent oxide (TCO), on which a thin metal grid (Ni-Al) is deposited, so as to reduce the series resistance of the window layer. The generally used TCO is zinc oxide (ZnO), the buffer layer is an N type semiconductor located between the absorbent layer and the optical window whose gap must be greater than that of the absorber; its thickness is around 50 nm. Two roles are mostly attributed to him: one role is electrical and the other is protective; from an electrical point of view, the buffer layer makes it possible, among other things, to optimize the alignment of the bands between the CIGS and the window layer and to limit the recombination of the carriers at the interface of these two layers. It also makes it possible to protect the surface of the absorber during the deposition by sputtering of the ZnO layer, which can cause the formation of defects on the surface of the CIGS [15].

The schematic diagrams of the two structures a shown in Fig. 2 and physical parameters of CZTS/CdS/ZnO and CIGS/CdS/ZnO solar cells, used in the simulation, are shown in Tables 1 and 2.

Table 1 – Front and back contact properties with series and shunts resistance of the two solar cells

Cell properties		
	CIGS Cell	CZTS Cell
Cell temperature	300 K	
Series resistance ($\Omega \cdot cm^{-2}$)	0.3 [2]	2 [6]
Shunt resistance ($\Omega \cdot cm^{-2}$)	3800 [2]	400 [6]
	Front metal contact properties	
Electron surface recombination velocity (cm/s)	1E7 [8]	1E7 [6, 7]
Hole surface recombination velocity (cm/s)	1E7 [8]	1E5 [6,7]
Metal work function (eV)	4.45 [8]	Flat band [6,7]
	Back metal contact properties	
Electron surface recombination velocity (cm/s)	1E7 [8]	1E5 [6,7]
Hole surface recombination velocity (cm/s)	1E7 [8]	1E7 [6,7]
Metal work function (eV)	5.4 [8]	5.5 [6]

Table 2 – Main material parameters CIGS/CdS/ZnO and CZTS/CdS/ZnO solar cell used in the simulation

Semiconductor parameter's	ZnO	CdS	CIGS	CZTS
Band gap (eV)	3.3 [8, 6]	2.4 [8, 6]	1.15 [8]	1.5 [6]
Dielectric permittivity (relative)	9[8, 6]	10 [8], 9 [6]	13.6 [8]	10 [6]
Electron mobility (cm^2/Vs)	100 [8, 6]	100 [8], 350[6]	100 [8]	100 [6]
Hole mobility (cm^2/Vs)	25 [8, 6]	25[8], 50[6]	25 [8]	25 [6]
NC effective density of states ($1/cm^3$)	2.2E18 [8, 6]	2.2E18 [8], 1.8E19[6]	2.2E18 [8]	2.2E18 [6]
NV effective density of states ($1/cm^3$)	1.8E19 [8, 6]	1.8E19 [8], 2.4E18[6]	1.8E19 [8]	1.8E19 [6]
Absorption coefficient (cm^{-1})	SCAPS data	SCAPS data	SCAPS data	2.5E4 [6]

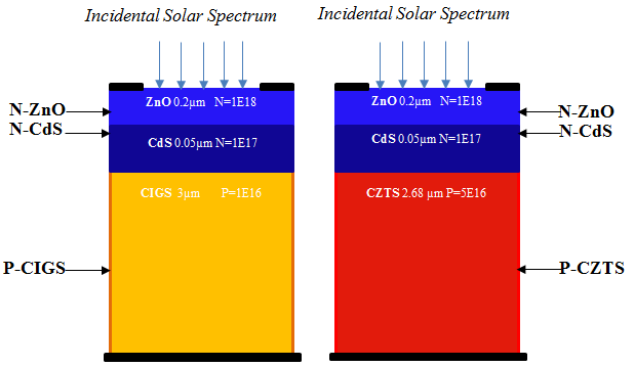

Fig. 2 – Structure of the CIGS/CdS/ZnO and CZTS/CdS/ZnO solar cells used in simulation

4. SIMULATION RESULTS

Before undertaking a comparative study between CZTS and CIGS solar cells for different temperature conditions, the application study has been begun by calibrating the two structures according to published results with light illumination of (1000 W/m^2) corresponding to AM1.5G global spectrum and temperature of 300 K.

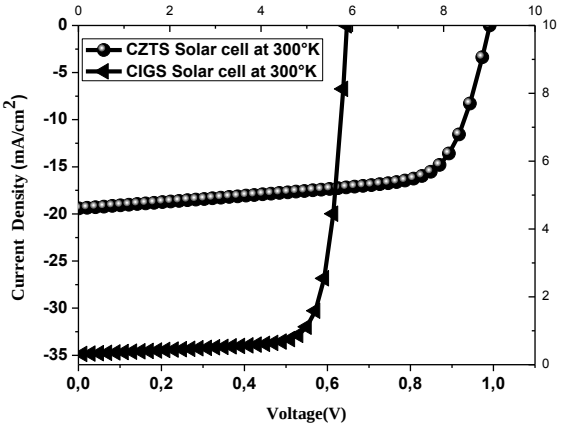

Fig. 3 – Comparison of simulated J-V characteristics of CZTS/CdS/ZnO and CIGS/CdS/ZnO under standard test conditions

The CZTS solar cell has been studied and optimized based on the optimized model of Malkeshkumar et al. 2012 [16]. The other CIGS cell has been optimized according to the experimental work given by Miguel in

Ref [17]. The simulation results allowed obtaining the $J(V)$ characteristics, which are compared to results of the optimized cell presented in Refs. [17] and [16] as shown in Table 3. The obtaining results are in good agreement with those obtained by the Refs. [2, 17, 16].

Table 3 – Comparison of simulated J-V characteristics of CZTS/CdS/ZnO and CIGS/CdS/ZnO with literature ref.

	Comparison	V_{oc} (Volt)	J_{sc} (mA/cm^2)	FF (%)	η (%)
CZTS-cell	SCAP-1D Simulation	0.991	19.42	68.7	13.19
	Optimized cell Ref[16]	1.002	19.31	69.35	13.41
CIGS-cell	SCAP-1D Simulation	0.646	34.89	78.03	17.55
	Experimental data Ref[17]	0.674	34	77	17.7

4.1 Temperature Effect on CZTS Solar Cell

In this section, a $J(V)$ characteristics of CZTS and CIGS based solar cells have been achieved in various temperatures ranged between 300 and 360 K.

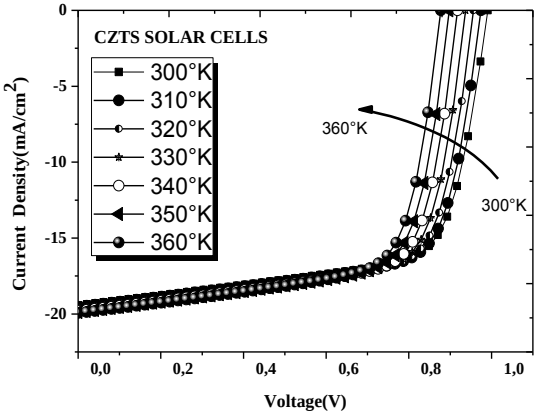

Fig. 4 – Temperature dependence of $J(V)$ characteristics of CZTS solar cell

Table 4– Performances of CZTS/CdS/ZnO solar cell at various temperatures

Temperature K- CZTS	V_{oc} (Volt)	J_{sc} (mA/cm^2)	FF (%)	η (%)
300	0,991	19,428	68,7	13,19
310	0,974	19,531	69,34	13,16
320	0,956	19,626	69,71	13,04
330	0,937	19,714	69,85	12,87
340	0,917	19,796	69,86	12,64
350	0,897	19,87	69,6	12,37
360	0,877	19,938	69,25	12,07

From Fig. 4 and Table 4, a remarkable reduction on the open circuit voltage and the conversion efficiency, accompanied with a slight increase in the short circuit current and the FF, has been registered. A decrease of 8.5 % in the conversion efficiency is noticed.

4.2 Temperature Effect on CIGS Solar Cell

For the CIGS solar cell, a very remarkable decrease has been obtained in the electrical parameter $J(V)$ (Fig. 5). The conversion efficiency of the solar cell decreased from 17.55 % to 12.89 %.

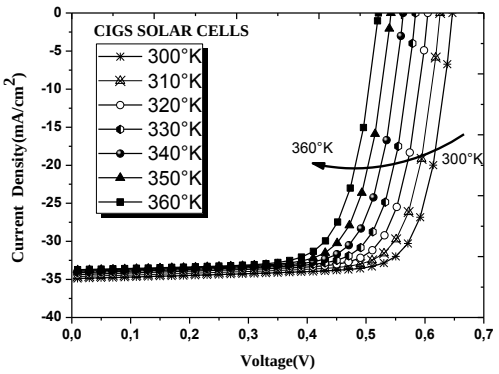

Fig.5 – Temperature dependence of $J(V)$ characteristics of CIGS solar cell

When the temperature increases, the observed diminution in the open circuit voltage (Fig. 4 and Fig. 5) is due to the increasing in the reverse saturation current density J_0; this increase of J_0 is mainly caused by the increase of the intrinsic carrier concentration ni and the decreasing in the band gap of the semiconductor material. Also, the increasing of cell temperature affects the material conductivity, which conducts to degradation of the solar cells performances.

Table 5 – Performances of CIGS /CdS/ZnO solar cell at various temperatures

Temperature, K- CIGS	V_{oc} (Volt)	J_{sc} (mA/cm^2)	FF (%)	η (%)
300	0,646	34,89	78,02	17,55
310	0,625	34,638	77,25	16,7
320	0,605	34,37	76,55	15,87
330	0,584	34,128	75,9	15,08
340	0,563	33,945	75,21	14,33
350	0,542	33,819	74,44	13,61
360	0,521	33,734	73,57	12,89

4.3 Comparison Study

In order to study the behavior of the two solar cells (CIGS and CZTS) with respect to temperature variation, a normalized value of solar cell performance has been examined as a function of temperature. The obtained results, illustrated in Figs. 6-10, show that CZTS solar cell have a good behavior at high temperature condition in comparison with CIGS solar cell. The linear decrease of V_{oc} and η (conversion efficiency) with increasing temperature could be explained by an increase in the darkness current with temperature Fig 6. When temperature increases, the band gap becomes narrower; the electrons-holes pair's recombination process, between the conduction and valence bands, is then accelerated and leads to an increasing in the darkness current in the cell. The coefficient of the voltage variation to temperature $\Delta V_{oc}/\Delta T$ of CIGS and

CZTS respectively are 0.0021 volt/ K and 0.0017 volt/ K. However, The FF also showed a tendency as similar as that of J_{sc} (Fig 7 and 8). The decreasing of FF and η with increasing temperature and efficiency degradation is mainly due to decrease in V*oc.* For CZTS structure, an improvement of FF has been achieved when temperature increases, which is in opposition with behavior of CIGS solar cell.

The decrease in maximum power of CZTS and CIGS solar cells are, respectively – 1.8 mW/cm² K and – 7.84 mW/cm² K, as shown in Table 6.

Table 6– Coefficient of the maximum power to temperature of CZTS and CIGS solar cells

	CZTS	CIGS
$\Delta P_{MAX} / \Delta T$ (mw/cm²/ K)	– 1.8	– 7.84

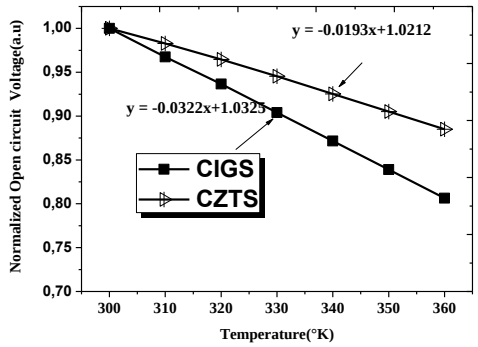

Fig. 6 – Normalized output open circuit voltage of CZTS and CIGS solar cells as a function of temperature

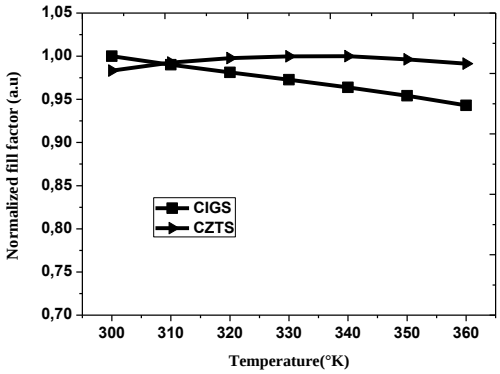

Fig. 7 – Normalized output FF of CZTS and CIGS solar cells as a function of temperature

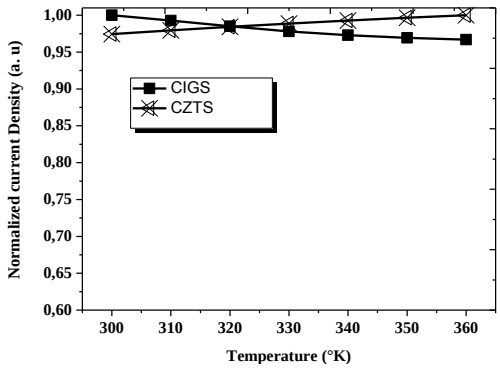

Fig. 8 – Normalized output current density of CZTS and CIGS solar cells as a function of temperature

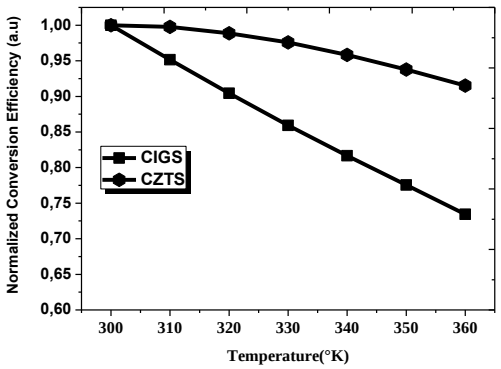

Fig. 9 – Normalized output conversion efficiency of CZTS and CIGS solar cells as a function of temperature

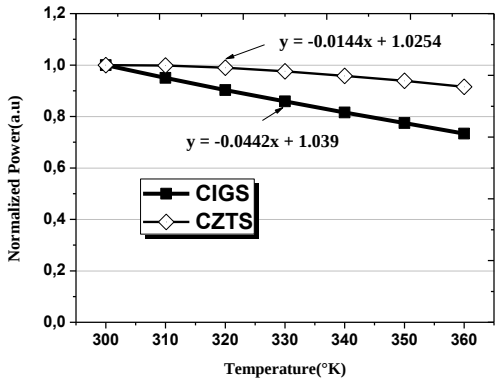

Fig. 10 – Normalized output maximum power of CZTS and CIGS solar cells as a function of temperature

5. CONCLUSION

In this paper, we carried out a comparative study on the effect of temperature on performance of CIGS/CdS/ZnO and CZTS/CdS/ZnO thin film solar cells. Its effect on the solar cell parameters such as the open-circuit voltage (V_{oc}), the short-circuit current density (J_{SC}) and the conversion efficiency ŋ has been demonstrated. Simulation results showed a better behaviour of CZTS/CdS/ZnO in comparison with CIGS/CdS/ZnO solar cell. Moreover, the coefficient ($\Delta P_{max}/\Delta T$) in CZTS/CdS/ZnO became very small in comparison with CIGS/CdS/ZnO. These results boost the use of CZTS material in the manufacturing of photovoltaic modules expected to work at high temperatures.

AKNOWLEDGEMENTS

The authors wish to thank Dr. M. Burgelman's group of Electronics and Information Systems (ELIS). University of Gent for the SCAPS-1D program tool.

REFERENCES

1. A.Mc. Evoy, T. Markvart, L. Castaner, *Practical Handbook of Photovoltaics Fundamentals and Applications, Second Edition* (Elsevier Ltd: 2012).
2. A. Morales-Acevedo, *Solar cells, Research and application perspectives* (Arturo Morales-Acevedo: 2013).
3. M.A. Green, K. Emery, Y.Hishikawa, W.Warta, E.D. Dunlop, *Prog. Photovolt: Res. Appl.* **24**, 905 (2016).
4. M. Yamaguchi, T. Takamoto, K. Araki, N. Ekins-Daukes, *Sol. Energ.* **79**, 78 (2005).
5. X. Jiaxiong, *J. Phys. Chem. Solids* **98**, 32 (2016).
6. I. Kentaro, *Copper Zinc Tin Sulfide-Based Thin-Film Solar Cells* (John Wiley & Sons. Ltd: 2015).
7. M. Danilson, E. Kask, N. Pokharel, G. Maarja, K.K. Marit, T. Varema, J. Krustok, *Thin Solid Films* **582**, 162 (2015).
8. C. Wadia, A. Alivisatos, D. Kammen, *Environ. Sci. Technol.* **43**, 2072 (2009).
9. J.J. Scragg, *Copper Zinc Tin Sulfide Thin Films for Photovoltaics* (Springer Theses, Springer-Verlag Berlin Heidelberg: 2011).
10. L.L. Kazmerski, *J. Electron Spectroscopy Related Phenomena* **150**, 105 (2006).
11. M.A. Green, K. Emery, Y. Hishikawa, W. Warta, E.D. Dunlop, *Prog. Photovolt:Res. Appl.* **23**, 805 (2015).
12. N. Kahoul, M. Houabes, M. Sadok, *Energy Conversion Management*. **82**, 320 (2014).
13. O.K. Simya, A. Mahaboobbatcha, K. Balachander, *Superlattice. Microstructure*. **82**, 248 (2015).
14. A. Goetzberger, J. Knobloch, B. Vob, *Crystalline Silicon Solar Cells* (John Wiley & Sons: 1998).
15. Kasturi Lal Chopra, Suhit Ranjan Das, *Thin Film Solar Cells* (Springer Science: 1983).
16. Patel M. Ray A, *Physica B* **407**, 4391(2012).
17. A.C. Miguel, E. Brian, K. Ramanathan. J. Hiltner. A. Swartzlander., F. Hasoon, N. Rommel, *Prog. Photovol: Res. Appl.* **7**, 311 (1999).